

MOL #30700

Subunit-specific Roles of Glycine-Binding Domains in Activation of NR1/NR3 “NMDA” Receptors

**Marc Awobuluyi¹, Jin Yang², Yuzhen Ye, Jon E. Chatterton³, Adam Godzik, Stuart A.
Lipton, and Dongxian Zhang**

Center for Neurosciences and Aging (M.A., J.Y., J.E.C., S.A.L., D.Z) and Center for Infectious
Diseases (Y.Y., A.G.), Burnham Institute for Medical Research, 10901 North Torrey Pines Road,
La Jolla, California 92037, USA.

MOL #30700

Running Title: Subunit-specific activation of NR1/NR3 receptors

Corresponding author

Dongxian Zhang, Burnham Institute for Medical Research

10901 N. Torrey Pines Road, La Jolla, CA 92037.

E-mail: dzhang@burnham.org

Tel# (858) 795-5263

Fax# (858) 795-5273

Total number of pages: 29

Total number of figures: 7

Total number of references: 40

Total number of words in:

- the Abstract: 195
- the Introduction: 648
- the Discussion: 812

Abbreviations:

AMPA, alpha-amino-3-hydroxy-5-methyl-4-isoxazolepropionic acid; ACPC, 1-Aminocyclopropane-1-carboxylic acid; 5,7-DCKA, 5,7-dichlorokyurenic acid; DTT, dithiothreitol; iGluRs, glutamate receptors; HEK, human embryonic kidney; MDL, MDL 105,519 [(E)-3-(2-phenyl-2-carboxyethenyl)-4,6-dichloro-1 H-indole-2-carboxylic acid]; MTS, methanethiosulfonate; MTSEA, 2-aminoethyl methanethiosulfonate; NMDARs, *N*-Methyl-D-aspartate receptors; SCAM, cysteine-scanning mutagenesis.

MOL #30700

Abstract

NMDA receptors (NMDARs) comprised of NR1 and NR3 subunits differ from other NMDAR subtypes in that they require glycine alone for activation. However, little else is known about the activation mechanism of these receptors. Using NMDAR glycine-site agonists/antagonists in conjunction with functional mutagenesis of the NR1 and NR3 ligand-binding cores, we demonstrate quite surprisingly that agonist binding to NR3 alone is sufficient to activate a significant component of NR1/NR3 receptor currents. Thus, the apo conformation of NR1 in NR1/NR3 receptors is permissive for receptor activation. Agonist-bound NR1 may also contribute to peak NR1/NR3 receptor currents, but specifically enables significant NR1/NR3 receptor current decay under the conditions studied here, presumably via a slow component of desensitization. Ligand studies of NR1/NR3 receptors also suggest differential agonist selectivity between NR3 and NR1, as some high affinity NR1 agonists activate NR1/NR3 receptors only poorly, whereas other NR1 agonists are as potent as glycine. Furthermore, liganded NR3 subunits appear necessary for effective engagement of NR1 in NR1/NR3 receptor activation, suggesting significant interactivity between the two subunits. NR3 subunits thus induce plasticity in NR1 with respect to subunit assembly and ligand binding/channel coupling that is unique amongst ligand-gated ion channel subunits.

MOL #30700

Introduction

N-Methyl-D-aspartate receptors (NMDARs) are a subtype of ionotropic glutamate receptors (iGluRs) that serve critical functions in physiological and pathological processes in the nervous system, including neuronal development, plasticity and neurodegeneration (Cull-Candy et al., 2001; Lipton and Rosenberg, 1994). NR1 and NR2A-D subunits co-assemble (Meguro et al., 1992; Monyer et al., 1992) to form conventional NMDARs whose activation requires glycine and glutamate as co-agonists (Kleckner and Dingledine, 1988). Conventional NMDARs comprised of NR1 and NR2A-D subunits also manifest high permeability to calcium, and exhibit strong voltage-dependent magnesium block. Like NR2 subunits, NR3A-B subunits require NR1 for functional assembly (Chatterton et al., 2002). However, in contrast to NR2 subunits, NR3A-B subunits co-assemble with NR1 to form excitatory glycine receptors, as they require glycine alone for activation, in the absence of glutamate or NMDA (Chatterton et al., 2002). Receptors comprised of NR1 and NR3 subunits desensitize at high glycine concentrations, are less permeable to calcium, and are relatively resistant to magnesium block (Chatterton et al., 2002). NR3 subunits bind glycine with very high affinity (Yao and Mayer, 2006). Additionally, when co-expressed with NR1 and NR2 subunits in heterologous cells, NR3 subunits modulate NMDAR activity by decreasing subunit conductance, Ca^{2+} permeability, and Mg^{2+} sensitivity (Chatterton et al., 2002; Ciabarra et al., 1995; Matsuda et al., 2002; Nishi et al., 2001; Pérez-Otaño et al., 2001; Sasaki et al., 2002; Sucher et al., 1995).

NR3A and NR3B subunits differ primarily with respect to their regional and developmental expression, as well as the glycine agonist binding sensitivities of the receptors into which they assemble (Chatterton et al., 2002; Ciabarra et al., 1995; Matsuda et al., 2002; Nishi et al., 2001; Sasaki et al., 2002; Sucher et al., 1995). Mice genetically lacking NR3A also manifest increased NMDA-induced currents and dendritic spine density (Das et al., 1998).

MOL #30700

A number of studies have suggested that iGluRs, including NMDARs, are tetrameric complexes (Chen et al., 1999; Rosenmund et al., 1998; Safferling et al., 2001). Recent crystallographic, electrical macroscopic, and biophysical studies have further demonstrated that two sets of agonist-binding domains within alpha-amino-3-hydroxy-5-methyl-4-isoxazolepropionic acid (AMPA) receptors assemble to form a dimer of two-fold symmetry (Armstrong and Gouaux, 2000; Nakagawa et al., 2005; Sun et al., 2002). In contrast, conventional NMDARs are comprised of NR1/NR2 heterodimers (Furukawa, et al, 2005), and studies with tandem NR1 and NR2A subunits expressed in HEK cells suggest that NMDARs assemble as non-symmetric 1-2 and 2-1 dimers around the channel, with a pair of NR1 subunits facing a pair of NR2 subunits (Schorge and Colquhoun, 2003). Additionally, patch-clamp recordings of single recombinant NR1/NR2B receptors suggest that NR1 and NR2 subunits control kinetically distinct components of gating, and undergo separate conformational changes upon agonist binding that precede opening of the channel pore (Banke and Traynelis, 2003). The prevailing model for activation of conventional NMDARs suggests that binding of glycine and glutamate to NR1 and NR2, respectively (Anson et al., 1998; Kuryatov et al., 1994), induces closure of the ligand-binding domains (Furukawa and Gouaux, 2003). The action of each ligand-binding domain is then transduced in a concerted manner through a membrane-spanning region of the NMDAR channel complex (M3 domain), whose rotation is ultimately implicated in channel opening (Jones et al., 2002; Sobolevsky et al., 2002a). In contrast, there is evidence that certain AMPA and kainate iGluRs may have subunit-specific channel gates that can independently operate in response to agonist binding (Rosenmund et al., 1998; Smith and Howe, 2000; Swanson et al., 2002). The activation mechanisms of NR1/NR3 receptors, however, are completely unknown.

MOL #30700

Here, we provide evidence that agonist binding to NR3 alone is able to activate NR1/NR3 receptors. In the presence of NR3 ligand binding, unliganded NR1 is permissive for a significant component of NR1/NR3 receptor activation, whereas concomitant glycine binding to NR1 induces marked decay of NR1/NR3 receptor currents, presumably via a slow component of desensitization. Thus, unlike other NMDARs, NR1/NR3 receptors manifest non-concerted receptor activation.

MATERIALS AND METHODS

In vitro cDNA mutagenesis. The amino acid residues for NR1 and NR3 subunits are numbered based on the sequences of the immature polypeptides. Point mutations were generated with a QuickChange Site Directed Mutagenesis Kit (Stratagene, La Jolla, CA). Positive clones were confirmed via sequencing.

Electrophysiological recording. Wild-type NR1, NR2A, NR3A, NR3B, and mutant NR1, NR3A, and NR3B cRNAs were produced using mMessage mMachine kits (Ambion). Oocytes were co-injected with 2 ng of NR1 and 4 ng of NR2A, or 12 ng of NR3A/B. Mutant cRNAs were injected at the same concentration as wild type. Recordings were performed 2-7 days after injection. Two electrode voltage-clamp recordings were performed at -80 mV in bath solution containing (in mM): 90 NaCl, 1 KCl, 1.5 BaCl₂, and 10 HEPES buffer (pH 7.5).

Recordings were obtained from 3 - 15 oocytes per experiment. Steady-state current responses (equilibrium currents after full current decay) were normalized internally to account for amplitude variation among oocytes. Data points represent mean \pm standard error. Drug dose-inhibition curve was derived by Prism 4 program using the modified Hill equation, $I/I_{max} = 1/(1 + [C]/IC_{50})^n$, where $[C]$ is the drug concentration and n is the Hill coefficient. The statistical significance of the difference between two data groups was analyzed by Student's t -test.

MOL #30700

Methanethiosulfonate (MTS)-containing solutions were prepared, stored, and applied as described (Karlin and Akabas, 1998). Drugs and their sources were as follows: MTS reagents from Toronto Research Chemicals, Inc. (Toronto, Canada); glycine, 5,7-DCKA, MDL from Tocris (Avonmouth, UK); D-glutamate, D-serine, NMDA, ACPC from Sigma-Aldrich (St. Louis, MO).

Molecular Modeling. The structure of the NR3B S1S2 ligand-binding core was modeled using the X-ray structure of a homologous domain from NR1 receptor (PDB code 1pb8) as a template. Modeller (Marti-Renom et al., 2000) was used to build the model, using the alignment derived by FFAS program (Rychlewski et al., 2000). The structures of NR1 and NR3 complexes with different ligands were predicted using the Autodock program (Morris et al., 1988). We first tested the performance of Autodock on these systems by predicting the complex structure of NR1 with glycine using the NR1 X-ray structure (Furukawa and Gouaux, 2003) with glycine removed and limiting the search space to docking in the known binding pocket. The predicted complex was very similar to the experimental one, differing only with respect to one hydrogen bond. An additional hydrogen bond between arginine 523 and glycine was predicted by the Autodock model instead of the hydrogen bond between glycine and the hydroxyl group of serine 688 in the NR1 crystal structure.

RESULTS

Interruption of NR1 Glycine Binding Potentiates NR1/NR3 Receptor Steady-State Currents

As previously demonstrated in oocytes (Chatterton et al., 2002), glycine-evoked responses of NR1/NR3B receptors progressively decayed with increasing agonist concentration (Fig. 1A).

MOL #30700

Due to concordant activation and current decay, the dose-response of NR1/NR3 receptors could not be adequately fit by the Hill equation to determine the number of binding sites and EC_{50} . However, as glycine binding to NR1 is central to NR1/NR2 receptor activation, we hypothesized that NR1/NR3 receptors may also be activated via NR1-glycine binding, with NR3 subunits playing a modulatory role. In order to examine the contribution of NR1 glycine binding to NR1/NR3 receptor activation, we mutated several NR1 S1S2 amino acid residues that have previously been demonstrated to be important in agonist sensitivity (Kuryatov et al., 1994).

NR1 Phe484 has been suggested to form a “lid,” sterically preventing bound agonist from leaving the closed cleft conformation (Furukawa and Gouaux, 2003), and mutation of Phe484 to alanine drastically reduces the sensitivity of NR1/NR2B receptors (*fold increase in glycine EC_{50} : ~6,350*; Kuryatov et al., 1994). Surprisingly, NR1(F484A)/NR3B demonstrated only minimal reduction in apparent glycine sensitivity, but in contrast to wild-type NR1/NR3B receptors, displayed dramatic potentiation of steady-state currents, with no apparent current decay even at the highest glycine concentrations (Fig. 1B). The relative steady state current potentiation at each agonist concentration was quantified as the ratio of glycine-evoked steady state currents normalized to the steady state response at 10 μ M glycine ($I/I_{10\mu M}$). The $I_{100\mu M}/I_{10\mu M}$ of NR1(F484A)/NR3B receptors was 19.2 ± 4.1 , whereas that of wild-type NR1/NR3B receptors was only 0.20 ± 0.02 (Fig. 1C). In contrast, NR1(F484A)/NR2A receptors evoked no detectable current in response to co-application of 200 μ M NMDA and up to 1 mM glycine (not shown).

Receptors containing NR1(D481K,E483K) or NR1(Q405K), each of which markedly attenuates NR1 glycine sensitivity (*fold increase in Q405K glycine EC_{50} : 14,200*; Kuryatov et al., 1994), also demonstrated large potentiation of steady-state currents, with minimal loss of

MOL #30700

apparent glycine sensitivity (Fig. 1C). NR1(Q405K) was omitted from the graphical representation in Fig. 1C as it evoked little or no current with 10 μ M glycine when co-expressed with NR3B. NR1(D481K,E483K)/NR3B and NR1(Q405K)/NR3B receptors demonstrated an $I_{100 \mu\text{M}}/I_{10 \mu\text{M}}$ value of 7.5 ± 1.8 and an $I_{100 \mu\text{M}}/I_{30 \mu\text{M}}$ value of 5.4 ± 0.6 , respectively. The $I/I_{10 \mu\text{M}}$ ratio between mutant (apart from NR1(Q405K)/NR3B) and wild-type receptors was statistically different (Student's *t*-test, $p < 0.05$) for all glycine concentrations equal to or greater than 30 μ M, but not at concentrations below 10 μ M. The mild loss of glycine sensitivity demonstrated by receptors comprised of NR1(F484A), NR1(D481K,E483K), or NR1(Q405K) subunits co-assembled with NR3B (Fig. 1C) mirrors the altered glutamate sensitivity reported for NR2B when co-assembled with these NR1 mutants (Kuryatov et al., 1994). Co-assembly of NR3A with each of these NR1 mutants demonstrated similar results (not shown). Collectively, each of the preceding NR1 S1S2 mutants potentiated steady-state currents in NR1/NR3 receptors by attenuating the normally manifested current decay, which presumably reflects a slow component of desensitization.

The preceding NR1 mutants each alter glycine efficacy without directly disrupting the hydrogen bonds with which glycine coordinates within NR1 S1S2 (Furukawa and Gouaux, 2003). Thus, we next examined the effect of directly interrupting NR1 glycine binding on NR1/NR3 receptor activation, using NR1(D732N) mutant subunits. The carboxy group of Asp732 in NR1 forms direct hydrogen bonds with the α -amino group of glycine (Furukawa and Gouaux, 2003), and mutation of Asp to Asn significantly attenuates glycine sensitivity, without altering the EC_{50} of co-assembled NR2B (*fold increase in glycine EC_{50} : 14,500*; Williams et al., 1996). In comparison to wild-type NR1/NR3B receptors, NR1(D732N)/NR3B receptors also demonstrated marked potentiation of steady-state currents, although comparably less than that of

MOL #30700

the other NR1 S1S2 mutants examined ($I_{100\ \mu\text{M}}/I_{10\ \mu\text{M}}$ value of 4.1 ± 0.2 ; Fig. 1C). Thus, these data extend the findings obtained with the S1S2 mutants affecting NR1 efficacy by directly implicating NR1 glycine binding in the induction of NR1/NR3 receptor current decay. Notably, however, despite the alteration in NR1 glycine binding, NR1(D732N)/NR3B receptors demonstrated no apparent loss of glycine sensitivity compared with wild-type NR1/NR3B receptors (Fig. 1C, D).

In order to rule out the possibility that NR1(D732N) permanently altered the overall structure of NR1/NR3 receptors, we attempted to reproduce the potentiation of NR1/NR3 steady-state currents reversibly, by selectively restricting glycine access to NR1. Accordingly, we performed cysteine-scanning mutagenesis (SCAM) (Karlin and Akabas, 1998) around the NR1 binding pocket to identify NR1 mutants that would be amenable to covalent modification by methanethiosulfonate (MTS) reagents without significantly affecting the glycine EC_{50} when co-assembled with NR2A. We identified one such mutant, V689C, that lies within helix F at the lower lip of the NR1 glycine binding cleft, with its side chain directed towards the mouth of the pocket (Furukawa and Gouaux, 2003). NR1(V689C) displayed only a small increase in glycine EC_{50} ($6.6 \pm 1.2\ \mu\text{M}$) relative to wild-type NR1 when co-injected with NR2A. Consistently, glycine dose-response curves of NR1(V689C)/NR3A receptors were qualitatively similar to that of wild-type NR1/NR3A receptors (compare Fig. 2A-left tracing with left inset). After covalent modification with 2-aminoethyl MTS (MTSEA), designed to sterically inhibit NR1 glycine binding, NR1(V689C)/NR3A receptors demonstrated dramatic relief of current decay, with marked potentiation of steady-state currents, and no apparent loss of glycine sensitivity (Fig. 2A-center tracing). In contrast, steady-state currents of wild-type NR1/NR3A receptors were minimally inhibited by MTSEA treatment (relative post/pre MTSEA ratio = 0.89 ± 0.02). Co-

MOL #30700

application of 100 μ M glycine with MTSEA prevented NR1(V689C)/NR3A receptor current potentiation, demonstrating direct competition between glycine and MTSEA for access to the NR1 agonist binding cleft (Fig. 2A, right inset). However, at high (>100 μ M) glycine levels, some decay of NR1(V689C)/NR3A receptor current was still observed, suggesting that MTSEA modification did not completely block NR1(V689C) glycine binding. Removal of MTSEA by chemical reduction with dithiothreitol (DTT) re-approximated glycine-evoked NR1(V689C)/NR3A steady-state currents to pre-MTSEA levels (Fig. 2A –right tracing). In contrast to NR1(V689C)/NR3A receptors, MTSEA modified-NR1 (V689C)/NR2A receptors displayed marked reversible inhibition of glycine/NMDA-evoked peak currents (Fig. 2B).

Disruption of the NR3 S1S2 Domain Abolishes NR1/NR3 Receptor Activation

As our experimental results above using NR1 S1S2 mutants indicated the importance of glycine binding to NR3 in receptor activation, we directly tested the functional role of NR3 subunits in NR1/NR3 receptors. Using the predicted structural similarities between NR3 and NR1 subunits, we examined the activation of NR1/NR3 receptors containing NR3 S1 segment mutants designed to impair agonist sensitivity (Fig. 3A). NR1/NR3A(Y605A) mutant receptors, in contrast to receptors containing the homologous NR1 mutation and wild-type NR3A subunits, demonstrated marked loss of glycine sensitivity, with very small currents induced only at extremely high glycine concentrations (Fig. 3B). Similarly, NR1/NR3 receptors containing NR3A(E522K), NR3A(D602K,K604Q), or homologous NR3B S1 segment mutants (Fig. 3A) also displayed drastically reduced glycine sensitivity, or no detectable current at up to 10 mM glycine (data not shown).

An alternate explanation for the marked loss of glycine sensitivity with NR3 S1 mutants might be that the mutations conferred decreased NR3 protein expression or stability in oocytes.

MOL #30700

To exclude this possibility, we used the solved partial crystal structure for the NR1 ligand binding domain to construct an atomic model of the S1S2 region of NR3 (see Methods). Analysis of the model suggested that the overall folding pattern of NR3A/B may be very similar to NR1. We used this information to perform SCAM around the NR3A ligand-binding core in order to identify an NR3A mutant that could reversibly inhibit activation of NR1/NR3A receptors when modified by MTS reagents. NR1/NR3A(N635C) receptors, containing a cysteine mutation within the predicted anterior aspect of the NR3A ligand core, demonstrated rapid decay of glycine-evoked currents with steady-state amplitudes of less than 50 nA (not shown). In order to facilitate quantitative analysis of the MTS effect on NR3A(N635C), we co-injected this mutant with a second mutant that disrupts glycine binding to NR1, namely NR1(Q405K). NR1(Q405K)/NR3A(N635C) receptors demonstrated sizeable glycine currents that showed decay only at very high glycine concentrations (Fig. 3C-top). Consistent with the data from the mutagenic disruption of glycine binding to NR3 subunits, covalent modification of NR1(Q405K)/NR3A(N635C) receptors by MTSEA nearly abolished the glycine-evoked response (Fig. 3C-center, 3D). Removal of MTSEA by reduction with DTT restored glycine-evoked currents to essentially pre-MTSEA levels (Fig. 3C-bottom). Co-application of 100 μ M glycine with 2.5 mM MTSEA did not inhibit the MTSEA-mediated effect (not shown). NR1(Q405K)/NR3A receptor glycine currents were only moderately inhibited by MTS (post/pre MTS ratio = 0.68 ± 0.16 , $n=3$). The mean post/pre MTS ratio between NR1(Q405K)/NR3A(N635C) receptors and NR1(Q405K)/NR3A receptors was statistically different ($p < 0.01$). Taken together, the results from the reversible attenuation of NR3 glycine efficacy provide additional structural and functional support for an essential role of NR3 ligand binding in NR1/NR3 receptor activation.

NR1 Glycine Binding Site Antagonists Potentiate NR1/NR3 Receptor Currents

In order to further distinguish the subunit-specific contributions to NR1/NR3 receptor activation, we examined the effect of NR1 glycine site antagonists. The inhibitory actions of 5,7-dichlorokyurenic acid (5,7-DCKA) and MDL 105,519 [(E)-3-(2-phenyl-2-carboxyethenyl)-4,6-dichloro-1 H-indole-2-carboxylic acid] (MDL) against NR1 are well established (Kemp and Leeson, 1993), and the structural determinants for 5,7-DCKA binding to NR1 have been characterized (Furukawa and Gouaux, 2003). In contrast, no antagonists against the NR3 ligand binding domain have been characterized. We had previously reported that at glycine concentrations without manifest current decay, 5,7-DCKA and MDL inhibit NR1/NR3 receptor-mediated currents in a dose-dependent fashion (Chatterton et al., 2002). Surprisingly, we observed that at higher glycine concentrations, where rapid current decay occurred, application of 5,7-DCKA and MDL instead relieved NR1/NR3B receptor current decay, and potentiated NR1/NR3B steady-state currents (Fig. 4A and MDL data not shown). The potentiation was most striking at agonist concentrations above 100 μ M, with relatively high agonist/antagonist ratios. NR1/NR3A receptors displayed similar inhibitor-mediated potentiation of steady-state currents as NR1/NR3B receptors (not shown). In contrast, 5,7-DCKA and MDL inhibited NR1/NR2A receptors at these glycine concentrations (Fig. 4A-inset; effective IC_{50} = 4.71 ± 0.60 μ M for 5,7-DCKA at NR1/NR2A in the presence of 150 μ M glycine/200 μ M NMDA; n = 5).

At higher 5,7-DCKA concentrations (≥ 50 μ M), potentiation of fixed glycine-evoked NR1/NR3B steady-state currents declined relative to that observed at lower 5,7-DCKA concentrations (< 50 μ M; Fig. 4A,B). Due to the complex nature of this response, one cannot calculate an accurate affinity of 5,7-DCKA for NR1/NR3 receptors. However, the bi-modal effect of 5,7-DCKA on glycine-evoked NR1/NR3B currents suggested that this antagonist may

MOL #30700

bind to at least two sites of differing affinities, possibly on different subunits. To explore possible 5,7-DCKA binding to NR3 subunits, we utilized the NR1(F484A) mutant subunit. The binding of DCKA to NR1 has been shown to involve critical π stacking with the aromatic ring of Phe484 (Furukawa and Gouaux, 2003), such that mutation of Phe484 severely disrupts NR1 binding of 7-chlorokyurenic acid, an antagonist closely related to 5,7-DCKA (Kuryatov et al., 1994). We found that 150 μ M glycine evoked non-decaying currents at NR1(F484A)/NR3B (Fig. 4C) and NR1(F484A)/NR3A receptors (not shown). In the context of the marked attenuation of glycine efficacy reported for the NR1(F484A) subunit (Kuryatov et al., 1994), we interpret this finding as receptor activation induced largely through NR3 agonist binding. Application of 5,7-DCKA to NR1(F484A)/NR3B receptors, in contrast to its action at wild-type NR1/NR3B receptors, did not potentiate 150 μ M glycine-activated currents, but instead elicited dose-dependent inhibition (Fig. 4C,D; apparent $IC_{50} = 46.76 \pm 5.12 \mu$ M in the presence of 150 μ M glycine). The relative IC_{50} values for 5,7-DCKA in the presence of 150 μ M glycine were $4.71 \pm 0.60 \mu$ M vs. $46.76 \pm 5.12 \mu$ M for NR1/NR2A and NR1(F484A)/NR3B receptors, respectively, suggesting that 5,7-DCKA binds preferentially to NR1 subunits over NR3 subunits within NR1/NR3 receptors. This finding parallels the considerably greater 5,7-DCKA affinity observed for NR1 S1S2 relative to NR3A S1S2 (Yao and Mayer, 2006). The asymmetric binding of 5,7-DCKA at NR1/NR3 receptors may explain the observed antagonist-induced potentiation of NR1/NR3 steady-state currents.

Agonists Further Distinguish Functional Properties of Subunit Types Within NR1/NR3 Receptors

We hypothesized that the activation characteristics of NR1 and NR3 might also be distinguishable on the basis of selective affinities for known NR1 agonists. We first tested D-

MOL #30700

serine, an endogenous full agonist of NR1 with approximately 3-fold greater affinity than glycine (Kemp and Leeson, 1993; Schell et al., 1995). The greater affinity of D-serine for NR1 has been structurally ascribed to the presence of 3 additional hydrogen bonds in the D-serine-NR1 S1S2 co-crystal complex compared to that of glycine-coordinated NR1 (Furukawa and Gouaux, 2003). Previously, we had shown that D-serine evokes only very small or no detectable inward currents as an NR1/NR3 receptor agonist (Chatterton et al., 2002). In the context of strong D-serine affinity for NR1, we reasoned that the small steady-state currents evoked by D-serine at NR1/NR3B receptors and the absence of detectable inward currents at NR1/NR3A receptors might in part be due to robust NR1-induced current decay. This notion has also been suggested from binding studies of NR3A (Yao and Mayer, 2006). To test this possibility, we assessed the effect of D-serine at NR1(D732N)/NR3B receptors. D-Serine elicited an approximately 20-fold increase in relative steady-state currents at NR1(D732N)/NR3B receptors ($I_{100 \mu\text{M}}/I_{10 \mu\text{M}} = 6.3 \pm 0.9$) compared to NR1/NR3B receptors ($I_{100 \mu\text{M}}/I_{10 \mu\text{M}} = 0.30 \pm 0.09$) (Fig. 5A-bottom, 5B). In contrast to the apparent inhibition of glycine currents induced by D-serine at wild-type NR1/NR3B receptors (Chatterton et al., 2002, Fig. 5C-left, 5D), addition of D-serine potentiated glycine-evoked currents at NR1(D732N)/NR3B receptors (Fig. 5C-right, 5D). Furthermore, at NR1(D732N)/NR3B receptors, the sensitivities to glycine and D-serine were similar. On the other hand, the efficacy of glycine was approximately 4 to 6-fold greater than D-serine in a dose-response range where statistically little NR1(D732N) agonist binding is expected, and the evoked response would primarily be attributable to NR3B binding (Fig. 5E-left, 5F). This finding contrasts with the comparable efficacies of these NR1 agonists at NR1/NR2A receptors (Fig. 5E-right, 5F), and may reflect differences in the pharmacology of NR1 and NR3 subunits within NR1/NR3 receptors. Collectively then, these data support the notion that D-serine is a

MOL #30700

high-affinity agonist of NR3 (Yao and Mayer, 2006), but demonstrate that D-serine has a greater efficacy at NR1 than at NR3 subunits.

1-Aminocyclopropane-1-carboxylic acid (ACPC), a potent partial NR1 agonist with approximately 5-fold greater binding affinity than glycine (Kemp and Leeson, 1993; Marvizon et al., 1989; Nadler et al., 1988), was markedly less potent and efficacious than glycine as an agonist of NR1/NR3B receptors. In our system, the EC_{50} for ACPC at NR1/NR2A receptors in the presence of 100 μ M NMDA was $1.30 \pm 0.07 \mu$ M ($n = 6$), whereas the EC_{50} for ACPC at NR1/NR3B receptors was $> 100 \mu$ M. At NR1/NR3B receptors, small currents were detected upon application of 100 μ M ACPC, with no apparent current decay observed even at concentrations as high as 1 mM (Fig. 6A, 6B). Moreover, unlike the action of 5,7-DCKA on glycine-evoked NR1/NR3B currents, application of 20 μ M 5,7-DCKA completely inhibited 1 mM ACPC-induced currents, similar to the inhibitory effect observed with 5,7-DCKA on glycine-evoked currents at NR1(F484A)/NR3B receptors (compare Fig. 6A,B to Fig. 4C,D). In contrast to the effect of ACPC as an independent agonist of NR1/NR3B receptors, as little as 1 μ M ACPC induced apparent inhibition of glycine-evoked NR1/NR3B currents, indicating a very potent effect (Fig. 6C,E). Because of the particularly strong affinity of ACPC for NR1, we used the NR1(F484A) mutant (see Fig. 1B,D) to assess the contribution of NR1 to the ACPC-induced glycine current decay. At NR1(F484A)/NR3B receptors, 10 μ M glycine-evoked currents were unaffected by ACPC at concentrations up to 1 mM (Fig. 6D, E). NR1(D732N)/NR3B receptors demonstrated a similar attenuation of the ACPC effect, albeit less marked at higher ACPC concentrations (not shown). Thus, as with the action of D-serine at wild-type NR1/NR3B receptors, the mechanism for the reduction of glycine-evoked NR1/NR3B currents by ACPC is consistent with the notion of NR1-enabled current decay. Collectively

MOL #30700

then, the most parsimonious explanation for the effect of ACPC on NR1/NR3 receptors is that NR1 subunits are very sensitive to ACPC, while NR3 subunits are quite insensitive. In support of this conclusion, in independent ligand-binding studies, the NR1 S1S2 domain demonstrated greater affinity for ACPC than the NR3A S1S2 domain (Yao and Mayer, 2006).

DISCUSSION

Our data suggest that a component of NR1/NR3 receptor activation may be mediated by binding of agonist to NR3 alone. A direct role of NR3 subunits in NR1/NR3 receptor activation is in agreement with the reported high affinity of glycine for the NR3A S1S2 domain (Yao and Mayer, 2006). Agonist binding to NR1 may contribute to peak NR1/NR3 currents, but specifically enables significant NR1/NR3 receptor current decay under the conditions studied here. Thus, the glycine dose-response profile of NR1/NR3 receptors may be explained, in the context of a greater affinity of glycine for NR3 compared to NR1 (Yao and Mayer, 2006), by the predominant effect of NR3-induced receptor activation and concentration-dependent NR1-enabled current decay.

This activation scheme proposed for NR1/NR3 receptors is supported by the differential effects of excitatory glycine site agonists and antagonists at NR1 and NR3 subunits. For example, we show that asymmetric binding of 5,7-DCKA at NR1/NR3 receptors may account for the observed antagonist-induced potentiation of NR1/NR3 steady-state currents. High binding-site occupancy has traditionally been proposed to maximize the open probability of NMDARs. Our data instead suggest that selective removal of agonist from NR1 allows a larger number of NR1/NR3 channels to remain open, presumably by attenuating receptor desensitization. We also demonstrate that D-serine has a greater efficacy at NR1 than at NR3 subunits, suggesting rapid, NR1-enabled current decay as a central component of the apparent D-

MOL #30700

serine-mediated inhibition of glycine-evoked NR1/NR3 receptor currents. Furthermore, the absence of ACPC-induced current decay at NR1/NR3B receptors and the strong inhibitory effect of 5,7-DCKA on 1 mM ACPC-evoked currents suggest weak but preferential binding of ACPC to NR3B over NR1 in unliganded NR1/NR3 receptors. This also suggests that unliganded NR3 subunits may exert a significant degree of negative cooperativity on ligand binding and/or efficacy at NR1, as application of ACPC alone results in an apparent weak and non-decaying response of NR1/NR3B receptors, but, in contrast, a potent inhibitory effect when co-applied with a non-decaying concentration of glycine.

The data presented here for NR1/NR3 receptors bears striking similarities to that of certain AMPA and kainate receptors. GluR5/KA2 receptors, for example, can be activated by dysiherbaine-binding to GluR5 alone, without concomitant binding to KA2 subunits (Swanson et al., 2002). Subsequent glutamate binding to KA2 then enables significant GluR5/KA2 desensitization. Other structure-function similarities between NR1/NR3 receptors and non-NMDA iGluRs exist. For instance, AMPA/kainate subunits and NR3 subunits, in contrast to other NMDAR subunits, also share identical amino acid residues within the guanine nucleotide-binding site of domain 2. Furthermore, like kainate and AMPA receptors, which have been suggested to gate subconductance states through agonist binding to only two or three subunits (Rosenmund et al., 1998; Smith and Howe, 2000; Swanson et al., 2002), NR1/NR3 receptors display a single unitary but small conductance, consistent with predominant agonist binding to NR3 subunits (Chatterton et al., 2002; Pérez-Otaño et al., 2001; Sasaki et al., 2002).

We speculate that upon functional assembly with NR3 subunits, the role of NR1 S1S2 in regulating channel activity is effectively reversed compared to that of NR1 S1S2 within NR1/NR2 receptors. Under this scenario, NR1 adopts an open-cleft configuration that is

MOL #30700

permissive for a component of NR1/NR3 receptor activation (Fig. 7B). In contrast, NR1 assembled with NR2 subunits is inferred to adopt a functionally distinct apo state that requires agonist binding to both NR1 and NR2 subunits for the permissive conformational change that enables channel opening (Fig. 7A) (Banke and Traynelis, 2003). The present study, however, does not exclude the possibility that NR1 agonist binding may contribute to peak NR1/NR3 receptor currents.

Our new data on NR1/NR3 receptors define a functional plasticity of NR1 subunit assembly and ligand binding/channel coupling that has been hitherto unrecognized, and which appears to be unique amongst ligand-gated receptor subunits. Furthermore, the predominant effects of glycine binding to NR3 over NR1 for activation of NR1/NR3 receptors, as well as subtle differences in assembly of NR1 with NR2 and NR3 subunits, afford a novel model system for dynamically and more fully evaluating features of NMDARs not readily elucidated by NR1/NR2 physiology or currently-available crystal structures. *In vivo*, the functional dichotomy between NR1 and NR3 subunits would make NR1/NR3 receptors an ideal biosensor for glycine, whose concentration-dependent feedback inhibition mediated by NR1-induced current decay could potentially be regulated across a dynamic range by allosteric effectors of NR1, such as protons and polyamines (Kashiwagi et al., 1997). In agreement with the similarities described here between NR1/NR3 receptors and non-NMDA iGluRs, sequence data suggest that NR1 and NR3 subunits are the least divergent of NMDAR subunits from a putative common ancestor gene (Andersson et al., 2001). It is conceivable then that the increased cation selectivity, dual agonist requirement, and glutamate co-agonist specificity of NMDARs containing NR2 subunits may represent an evolutionary attempt to provide increased receptor selectivity in the setting of evolving complexity within the synaptic cleft.

MOL #30700

Acknowledgments

We thank Nobuki Nakanishi and Vincent H.-S. Chen for helpful discussions, and Jennifer Noerenberg for assistance with construction and preparation of NMDAR subunit mutants.

References

- Andersson O, Stenqvist A, Attersand A and von Euler G (2001) Nucleotide sequence, genomic organization, and chromosomal localization of genes encoding the human NMDA receptor subunits NR3A and NR3B. *Genomics* **78**(3):178-184.
- Anson LC, Chen PE, Wyllie DJ, Colquhoun D and Schoepfer R (1998) Identification of amino acid residues of the NR2A subunit that control glutamate potency in recombinant NR1/NR2A NMDA receptors. *J Neurosci* **18**(2):581-589.
- Armstrong N and Gouaux E (2000) Mechanisms for activation and antagonism of an AMPA-sensitive glutamate receptor: crystal structures of the GluR2 ligand binding core. *Neuron* **28**(1):165-181.
- Banke TG and Traynelis SF (2003) Activation of NR1/NR2B NMDA receptors. *Nat Neurosci* **6**(2):144-152.
- Chatterton JE, Awobuluyi M, Premkumar LS, Takahashi H, Talantova M, Shin Y, Cui J, Tu S, Sevarino KA, Nakanishi N, Tong G, Lipton SA and Zhang D (2002) Excitatory glycine receptors containing the NR3 family of NMDA receptor subunits. *Nature* **415**(6873):793-798.
- Chen GQ, Cui C, Mayer ML and Gouaux E (1999) Functional characterization of a potassium-selective prokaryotic glutamate receptor. *Nature* **402**(6763):817-821.
- Ciabarra AM, Sullivan JM, Gahn LG, Pecht G, Heinemann S and Sevarino KA (1995) Cloning and characterization of chi-1: a developmentally regulated member of a novel class of the ionotropic glutamate receptor family. *J Neurosci* **15**(10):6498-6508.
- Cull-Candy S, Brickley S and Farrant M (2001) NMDA receptor subunits: diversity, development and disease. *Curr Opin Neurobiol* **11**(3):327-335.
- Das S, Sasaki YF, Rothe T, Premkumar LS, Takasu M, Crandall JE, Dikkes P, Conner DA, Rayudu PV, Cheung W, Chen HS, Lipton SA and Nakanishi N (1998) Increased NMDA current and spine density in mice lacking the NMDA receptor subunit NR3A. *Nature* **393**(6683):377-381.
- Furukawa H and Gouaux E (2003) Mechanisms of activation, inhibition and specificity: crystal structures of the NMDA receptor NR1 ligand-binding core. *Embo J* **22**(12):2873-2885.
- Jones KS, VanDongen HM and VanDongen AM (2002) The NMDA receptor M3 segment is a conserved transduction element coupling ligand binding to channel opening. *J Neurosci* **22**(6):2044-2053.
- Karlin A and Akabas MH (1998) Substituted-cysteine accessibility method. *Methods Enzymol* **293**:123-145.
- Kashiwagi K, Pahk AJ, Masuko T, Igarashi K and Williams K (1997) Block and modulation of N-methyl-D-aspartate receptors by polyamines and protons: role of amino acid residues in the transmembrane and pore-forming regions of NR1 and NR2 subunits. *Mol Pharmacol* **52**(4):701-713.
- Kemp JA and Leeson PD (1993) The glycine site of the NMDA receptor--five years on. *Trends Pharmacol Sci* **14**(1):20-25.
- Kleckner NW and Dingledine R (1988) Requirement for glycine in activation of NMDA-receptors expressed in *Xenopus* oocytes. *Science* **241**(4867):835-837.
- Kuryatov A, Laube B, Betz H and Kuhse J (1994) Mutational analysis of the glycine-binding site of the NMDA receptor: structural similarity with bacterial amino acid-binding proteins. *Neuron* **12**(6):1291-1300.

MOL #30700

- Lipton SA and Rosenberg PA (1994) Excitatory amino acids as a final common pathway for neurologic disorders. *N Engl J Med* **330**(9):613-622.
- Marti-Renom MA, Stuart AC, Fiser A, Sanchez R, Melo F and Sali A (2000) Comparative protein structure modeling of genes and genomes. *Annu Rev Biophys Biomol Struct* **29**:291-325.
- Marvizon JC, Lewin AH and Skolnick P (1989) 1-Aminocyclopropane carboxylic acid: a potent and selective ligand for the glycine modulatory site of the N-methyl-D-aspartate receptor complex. *J Neurochem* **52**(3):992-994.
- Matsuda K, Kamiya Y, Matsuda S and Yuzaki M (2002) Cloning and characterization of a novel NMDA receptor subunit NR3B: a dominant subunit that reduces calcium permeability. *Brain Res Mol Brain Res* **100**(1-2):43-52.
- Meguro H, Mori H, Araki K, Kushiya E, Kutsuwada T, Yamazaki M, Kumanishi T, Arakawa M, Sakimura K and Mishina M (1992) Functional characterization of a heteromeric NMDA receptor channel expressed from cloned cDNAs. *Nature* **357**(6373):70-74.
- Monyer H, Sprengel R, Schoepfer R, Herb A, Higuchi M, Lomeli H, Burnashev N, Sakmann B and Seeburg PH (1992) Heteromeric NMDA receptors: molecular and functional distinction of subtypes. *Science* **256**(5060):1217-1221.
- Nadler V, Kloog Y and Sokolovsky M (1988) 1-Aminocyclopropane-1-carboxylic acid (ACC) mimics the effects of glycine on the NMDA receptor ion channel. *Eur J Pharmacol* **157**(1):115-116.
- Nakagawa T, Cheng Y, Ramm E, Sheng M and Walz T (2005) Structure and different conformational states of native AMPA receptor complexes. *Nature* **433**(7025):545-549.
- Nishi M, Hinds H, Lu HP, Kawata M and Hayashi Y (2001) Motoneuron-specific expression of NR3B, a novel NMDA-type glutamate receptor subunit that works in a dominant-negative manner. *J Neurosci* **21**(23):RC185.
- Pérez-Otaño I, Schulteis CT, Contractor A, Lipton SA, Trimmer JS, Sucher NJ and Heinemann SF (2001) Assembly with the NR1 subunit is required for surface expression of NR3A-containing NMDA receptors. *J Neurosci* **21**(4):1228-1237.
- Rosenmund C, Stern-Bach Y and Stevens CF (1998) The tetrameric structure of a glutamate receptor channel. *Science* **280**(5369):1596-1599.
- Rychlewski L, Jaroszewski L, Li W and Godzik A (2000) Comparison of sequence profiles. Strategies for structural predictions using sequence information. *Protein Sci* **9**(2):232-241.
- Safferling M, Tichelaar W, Kummerle G, Jouppila A, Kuusinen A, Keinänen K and Madden DR (2001) First images of a glutamate receptor ion channel: oligomeric state and molecular dimensions of GluRB homomers. *Biochemistry* **40**(46):13948-13953.
- Sasaki YF, Rothe T, Premkumar LS, Das S, Cui J, Talantova MV, Wong HK, Gong X, Chan SF, Zhang D, Nakanishi N, Sucher NJ and Lipton SA (2002) Characterization and comparison of the NR3A subunit of the NMDA receptor in recombinant systems and primary cortical neurons. *J Neurophysiol* **87**(4):2052-2063.
- Schell MJ, Molliver ME and Snyder SH (1995) D-serine, an endogenous synaptic modulator: localization to astrocytes and glutamate-stimulated release. *Proc Natl Acad Sci U S A* **92**(9):3948-3952.
- Schorge S and Colquhoun D (2003) Studies of NMDA receptor function and stoichiometry with truncated and tandem subunits. *J Neurosci* **23**(4):1151-1158.
- Smith TC and Howe JR (2000) Concentration-dependent substate behavior of native AMPA

MOL #30700

- receptors. *Nat Neurosci* **3**(10):992-997.
- Sobolevsky AI, Beck C and Wollmuth LP (2002a) Molecular rearrangements of the extracellular vestibule in NMDAR channels during gating. *Neuron* **33**(1):75-85.
- Sobolevsky AI, Rooney L and Wollmuth LP (2002b) Staggering of subunits in NMDAR channels. *Biophys J* **83**(6):3304-3314.
- Sucher NJ, Akbarian S, Chi CL, Leclerc CL, Awobuluyi M, Deitcher DL, Wu MK, Yuan JP, Jones EG and Lipton SA (1995) Developmental and regional expression pattern of a novel NMDA receptor-like subunit (NMDAR-L) in the rodent brain. *J Neurosci* **15**(10):6509-6520.
- Sun Y, Olson R, Horning M, Armstrong N, Mayer M and Gouaux E (2002) Mechanism of glutamate receptor desensitization. *Nature* **417**(6886):245-253.
- Swanson GT, Green T, Sakai R, Contractor A, Che W, Kamiya H and Heinemann SF (2002) Differential activation of individual subunits in heteromeric kainate receptors. *Neuron* **34**(4):589-598.
- Williams K, Chao J, Kashiwagi K, Masuko T and Igarashi K (1996) Activation of N-methyl-D-aspartate receptors by glycine: role of an aspartate residue in the M3-M4 loop of the NR1 subunit. *Mol Pharmacol* **50**(4):701-708.
- Yao Y and Mayer ML (2006) Characterization of a soluble ligand binding domain of the NMDA receptor regulatory subunit NR3A. *J Neurosci* **26**(17):4559-4566.

MOL #30700

Footnotes

This work was supported in part by NIH grants P01 HD29587, R01 EY05477, R01 EY09024, and R01 NS43434.

M.A and J.Y contributed equally to this article.

1. Current affiliation: Department of Neuroradiology, University of California, San Francisco, San Francisco, California, 94143, USA.

2. Current affiliation: Scripps Research Institute, 10901 North Torrey Pines Road, La Jolla, California 92037, USA.

3. Current affiliation: Alcon Research, Ltd., 6201 South Freeway, Fort Worth, Texas 76036, USA.

MOL #30700

Figure Legends

Fig. 1. NR1 S1S2 domain mutants markedly potentiate glycine-evoked steady-state currents when co-assembled with NR3 subunits. A, dose response of glycine-evoked NR1/NR3B currents. Large tail currents representing resensitization are seen upon washout of high concentrations of agonist. B, representative tracings of glycine dose response for NR1(F484A)/NR3B receptors. C, normalized steady state (I_{Eq}) glycine dose-response profiles ($\log(I_{Eq}/I_{Eq(10\ \mu M)})$) of NR1/NR3B, NR1(D732N)/NR3B, NR1(F484A)/NR3B, and NR1(D481K/K483E)/NR3B receptors. D, representative tracings of glycine dose response for NR1(D732N)/NR3B receptors. NR1(D732N)/NR3B receptors demonstrate similar apparent glycine sensitivity as wild-type NR1/NR3B receptors.

Fig. 2. MTS-mediated inhibition of NR1 glycine binding reproduces effects of NR1 S1S2 ligand mutations. A, (left inset) representative tracing of glycine-evoked dose responses for wild-type NR1/NR3A receptors. (left tracing) NR1(V689C)/NR3A receptors demonstrate a similar glycine dose response as wild-type receptors. (center tracing) Marked relief of current decay occurs after application of 2.5 mM MTSEA. The marked potentiation of NR1(V689C)/NR3A receptor steady state currents by MTSEA was reproducible across multiple (n=4) experiments. However, accurate quantification of potentiation was not possible due to the high sensitivity of NR1/NR3A and NR1(V689C)/NR3A to trace glycine in the bath solution. In this setting, steady-state currents at high glycine concentrations were at times of lower amplitude than “baseline” currents. (right inset) Co-application of 100 μ M glycine with 2.5 mM MTSEA prevents MTSEA-mediated glycine steady-state current potentiation. (right tracing) 5 mM DTT restored

MOL #30700

currents to pre-MTSEA levels. Arrowheads indicate start of wash after MTSEA or DTT incubations. B, (left) dose-response of NR1(V689C)/NR2A receptors pre-MTSEA treatment. (center), Marked attenuation of NR1(V689C)/NR2A receptor currents after application of 2.5mM MTSEA. (inset) Relative current response (post MTSEA/pre MTSEA) of NR1(V689C)/NR2A (black, n=8) and NR1/NR2A (grey, n=5) receptors at indicated glycine concentrations (current ratio: glycine-induced currents after vs. before MTSEA treatment). The current ratios between NR1(V689C)/NR2A and NR1/NR2A receptors were statistically different (**p<0.01) at all glycine concentrations tested. (right) 5 mM DTT approximates NR1(V689C)/NR2A receptor currents to pre-MTSEA levels.

Fig. 3. Functional characteristics of NR3 subunits. A, aligned NR3A/B and NR1 S1 domains with mutated residues shaded. Sequences are numbered according to the predicted NMDA subunit polypeptides. B, representative tracing (top) and dose response curve (bottom) from NR1/NR3A(Y605A) receptors manifesting marked loss of glycine sensitivity (other NR3 S1S2 domain mutants shaded in Fig. 3A displayed similar effects). C, (top) NR1(Q405K)/NR3A(N635C) receptors manifest a qualitatively similar glycine dose response as NR1(Q405K)/NR3A receptors. (middle) Application of 1 mM MTSET nearly abolished glycine-evoked activation of NR1(Q405K)/NR3A(N635C) receptors. (bottom) 5 mM DTT restored currents to pre-MTSET levels. Arrowheads indicate start of wash after MTSET or DTT incubation. D, quantification of relative current attenuation post 1mM MTSET treatment (current ratio: glycine-induced currents after vs. before MTSET treatment). The current ratio post MTSET treatment was statistically different from that before treatment (n=5, **p<0.01).

MOL #30700

Fig. 4. Effect of 5,7-DCKA on NR1/NR3B and NR1(F484A)/NR3B receptor steady-state currents. A, representative trace demonstrating dose-dependent potentiation of 150 μ M glycine-evoked steady-state currents by 5,7-DCKA on NR1/NR3B receptors. The largest potentiation was observed at high ratios of applied glycine relative to applied 5,7-DCKA. At the highest 5,7-DCKA concentrations, relative inhibition of 150 μ M glycine steady-state currents was observed compared to lower concentrations of 5,7-DCKA. (inset) Representative tracing of NR1/NR2A receptor inhibition (150 μ M glycine/200 μ M NMDA) by 20 μ M 5,7-DCKA. Slowed re-activation kinetics are apparent after 5,7-DCKA washout. B, 5,7-DCKA dose-response profile for NR1/NR3B receptors (n=4) in the presence of 150 μ M glycine (current ratio: combined 5,7-DCKA/glycine current normalized to 150 μ M glycine current alone (I_0)). C, representative tracing of 5,7-DCKA dose-response in the presence of 150 μ M glycine. D, 5,7-DCKA dose-response profile for NR1(F484A)/NR3B receptors (n=5) in the presence of 150 μ M glycine (current ratio as defined above).

Fig. 5. Effects of D-serine on wild-type NR1/NR3 and NR1(D732N)/NR3 receptors. A, (top) representative dose-response tracing of D-serine-evoked currents at NR1/NR3B receptors. (bottom) Dose response of D-serine-evoked currents on NR1(D732N)/NR3B receptors. B, current ratio (100 μ M:10 μ M agonist) of glycine-evoked (black) and D-serine-evoked (gray) steady-state currents on NR1/NR3B (n=5) and NR1(D732N)/NR3B (n=6) receptors. The current ratios between wild-type and mutant receptors were statistically different for both glycine and D-serine-evoked response (**p<0.01). Relative, rather than absolute, steady-state current amplitudes were assessed to circumvent possible variability between expression of wild-type and mutant NR1/NR3B receptors. C, representative dose-response of D-serine in the presence of

MOL #30700

fixed 10 μ M glycine on NR1/NR3B (left) and NR1(D732N)/NR3B receptors (right). D-Serine induced current decay of NR1/NR3B glycine currents, but potentiated glycine-evoked NR1(D732N)/NR3B receptor currents. D, quantification of D-serine effects on glycine-evoked currents at NR1/NR3B (n=5) vs. NR1(D732N)/NR3B receptors (n=6) (current ratio: combined D-serine/glycine current normalized to 10 μ M glycine current alone (I_0)). The current ratios between wild-type and mutant receptors were statistically different at 1 μ M, 10 μ M, and 100 μ M D-serine concentration (* $p < 0.05$, ** $p < 0.01$). E, representative tracing of glycine and D-serine dose responses on NR1(D732N)/NR3B receptors (left) and NR1/NR2A receptors (right) in a linear agonist-response range. F, current ratios of glycine- and D-serine-induced responses at NR1(D732N)/NR3B (n=3) and NR1/NR2A (n=4) receptors (equal concentrations of glycine and D-serine were applied; 200 μ M NMDA was added for NR1/NR2A receptors). The current ratios between NR1/2A and NR1(D732N)/NR3B receptors were statistically different (** $p < 0.01$) at each agonist concentration.

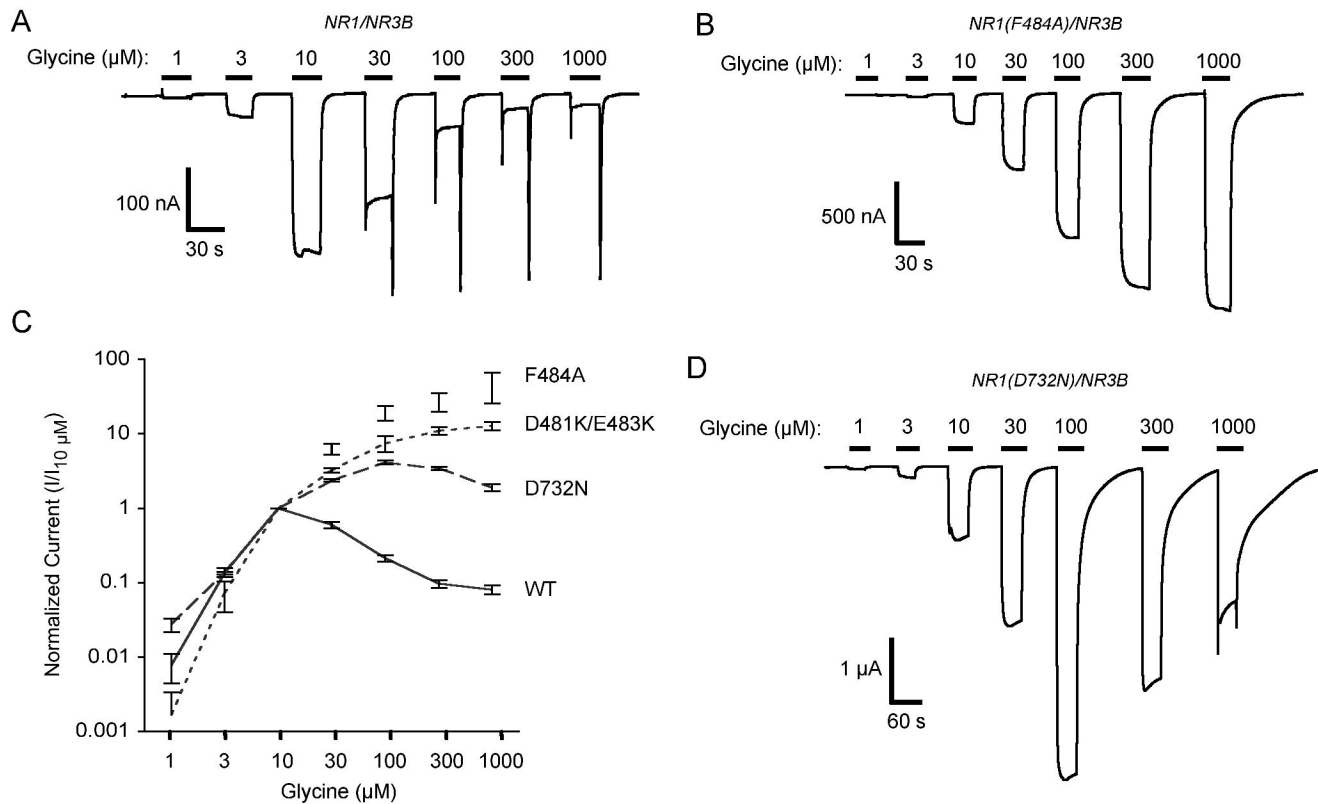
Fig. 6. Effect of ACPC on wild-type NR1/NR3 and NR1(F484A)/NR3B receptors. A, representative tracing from NR1/NR3B receptors comparing glycine- vs. ACPC-evoked currents. ACPC (right) was less effective and less potent than glycine (left) as an agonist of NR1/NR3B receptors and did not induced current decay; 20 μ M 5,7-DCKA completely inhibited, rather than potentiated 1 mM ACPC-evoked currents at NR1/NR3B receptors. B, quantitative comparison of ACPC-evoked currents (+/- 5,7-DCKA) at NR1/NR3B receptors normalized to 10 μ M glycine-evoked current (n=6). The 10 μ M, 100 μ M, and 1000 μ M ACPC-induced currents were all significantly smaller than 10 μ M glycine-induced currents (** $p < 0.01$). C, representative tracing of ACPC-induced current decay of NR1/NR3B glycine-evoked currents. D, Unlike its

MOL #30700

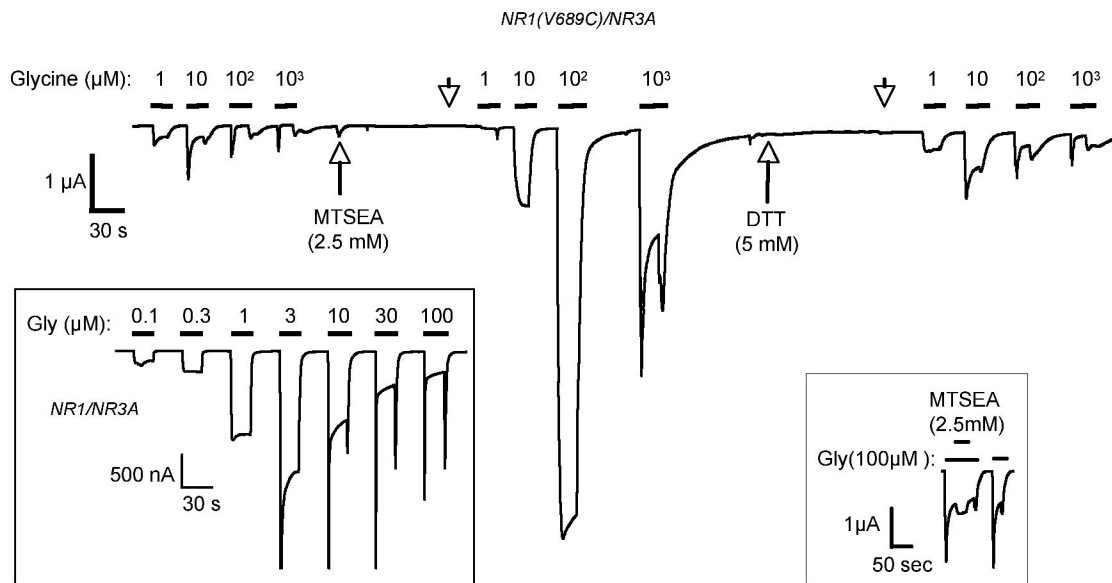
effect at wild-type NR1/NR3B receptors, ACPC (≤ 1 mM) did not induce current decay of 10 μ M glycine-evoked NR1(F484A)/NR3B currents. E, comparison of ACPC effects on glycine-evoked currents at NR1/NR3B (n=7) vs. NR1(F484A)/NR3B (n=7) receptors (current ratio: combined ACPC/glycine current normalized to 10 μ M glycine current alone (I_o)). The current ratios between NR1/NR3B and NR1(F484A)/NR3B receptors were statistically different (* $p < 0.05$, ** $p < 0.01$) at 10 μ M, 100 μ M, and 1000 μ M ACPC concentration.

Fig. 7. Schematic model for activation of NR1/NR3 receptors. A, simplified representation of NR1/NR2 receptor activation. The diagram depicts one subunit each from an NR1 dimer (blue) and an NR2 dimer (green) proposed to form NMDA receptors. The intra-membrane portion of the receptor is represented by single coils (for simplicity) that are not staggered (Sobolevsky et al., 2002b). The conformational changes that are proposed to precede channel opening but occur following binding of glycine and glutamate to NR1 and NR2, respectively, are also omitted for simplicity (Banke and Traynelis, 2003). B, simplified representation of NR1/NR3 receptor activation and current decay. One of two NR1/NR3 heterodimers inferred to form NR1/NR3 receptors is shown. (left) NR1 is predicted to adopt a unique “permissive” conformation upon assembly with NR3 subunits (steel). (center-left) Ligand binding to NR3 subunits alone is sufficient to activate a component of NR1/NR3 receptor currents. (center-right) Ligand binding to NR1 is inferred to destabilize NR1/NR3 receptors. (right) The conformational change associated with ligand binding leads to current decay.

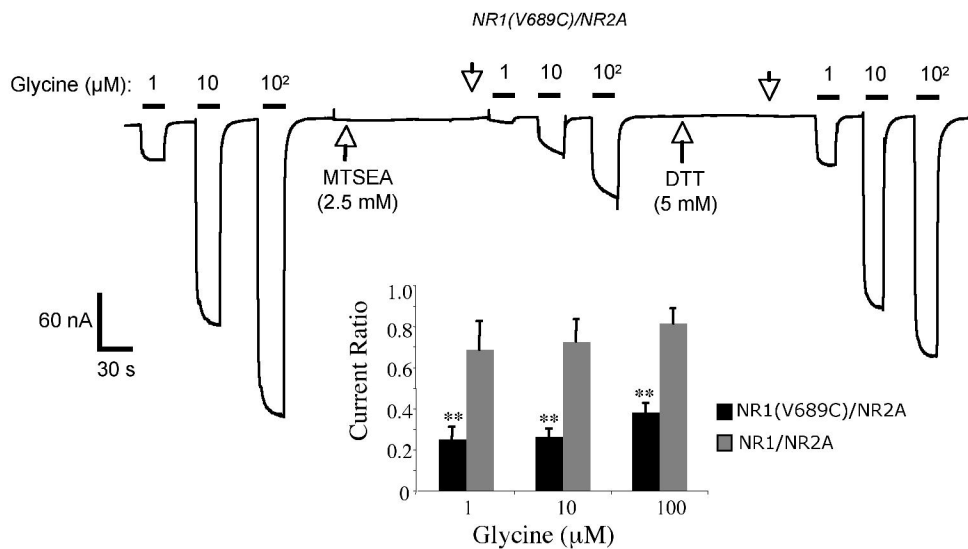
Figure 1

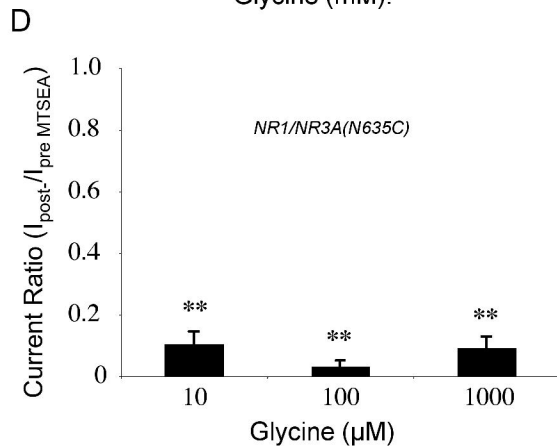
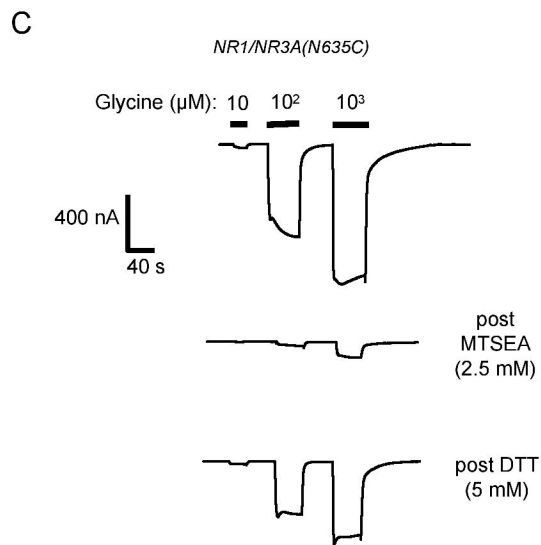
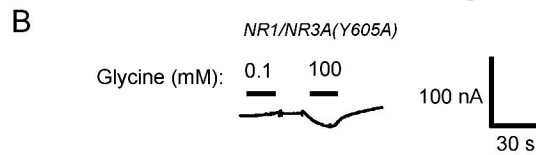
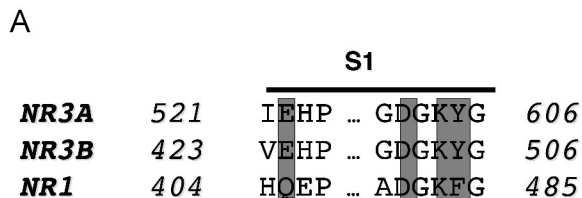


A

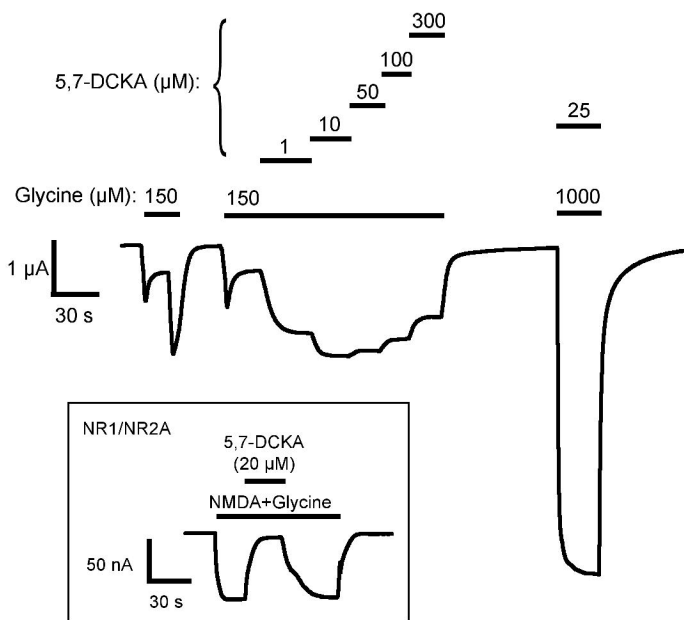


B

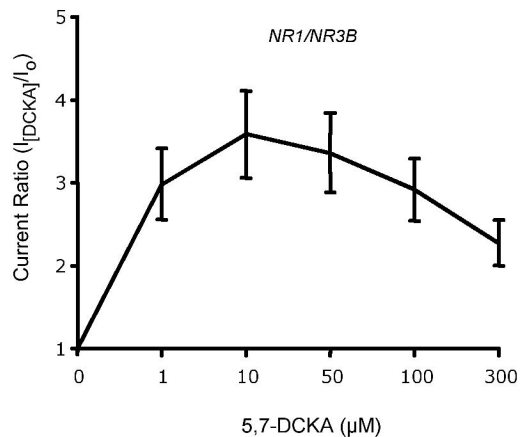




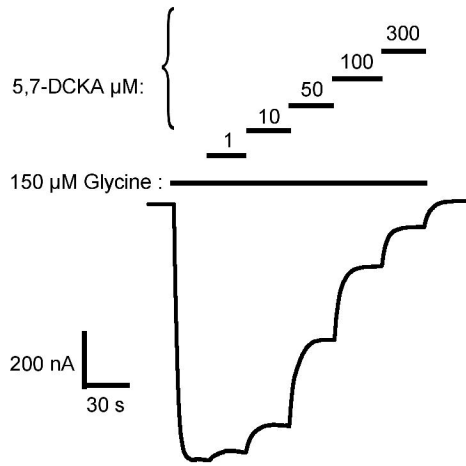
A

NR1/NR3B

B



C

NR1(F484A)/NR3B

D

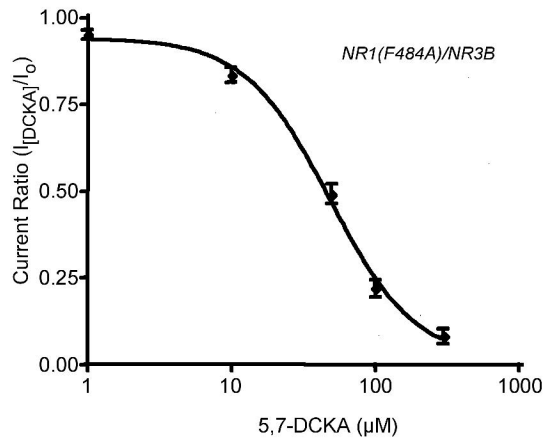
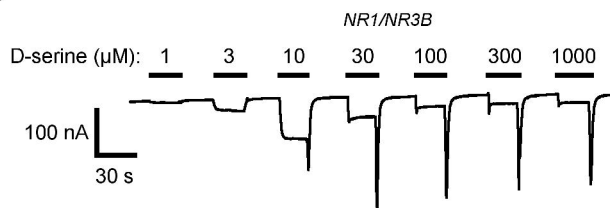
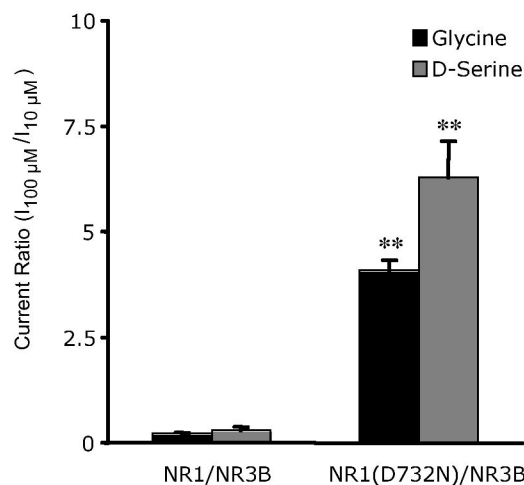


Figure 5

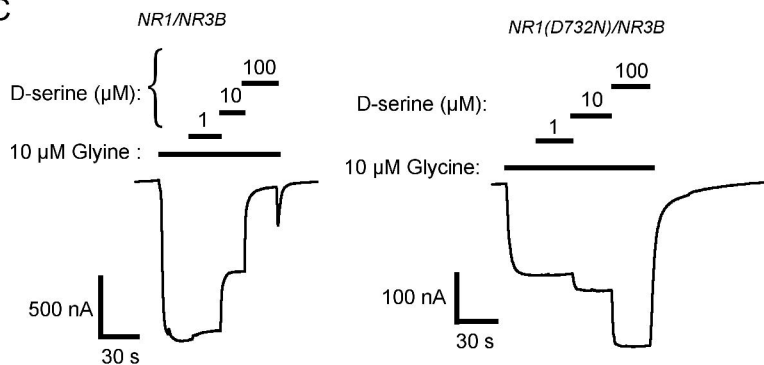
A



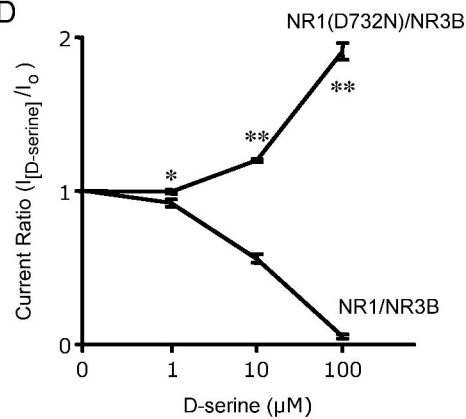
B



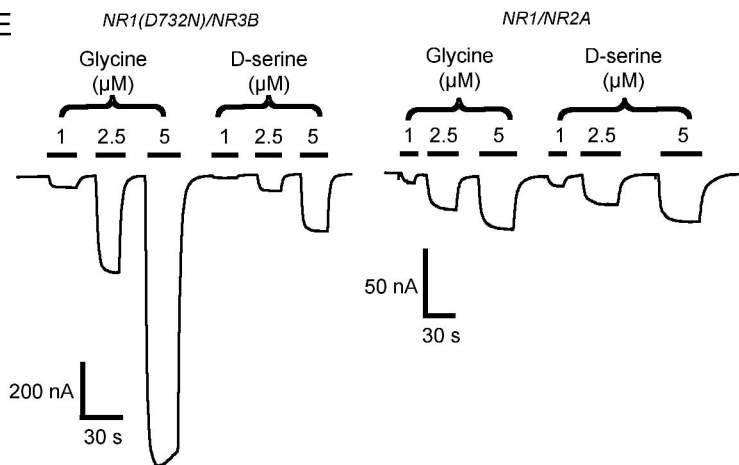
C



D



E



F

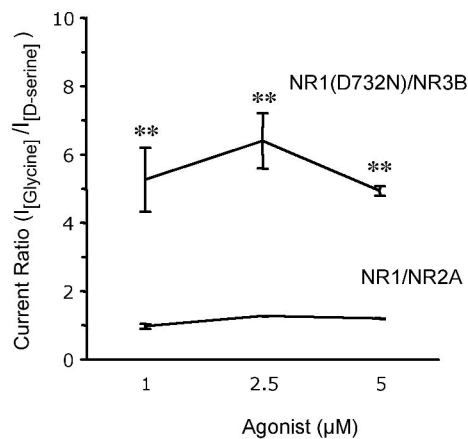
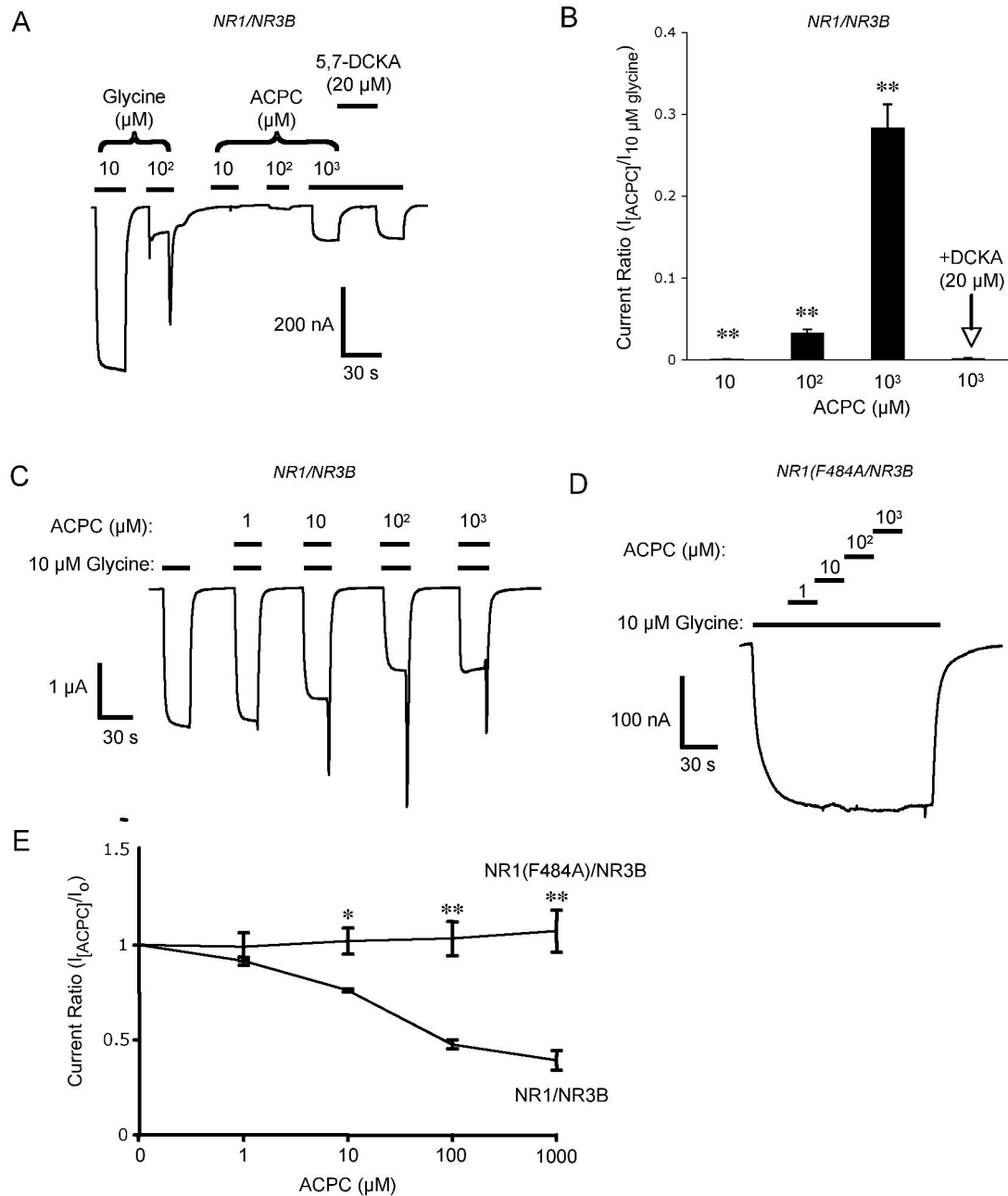
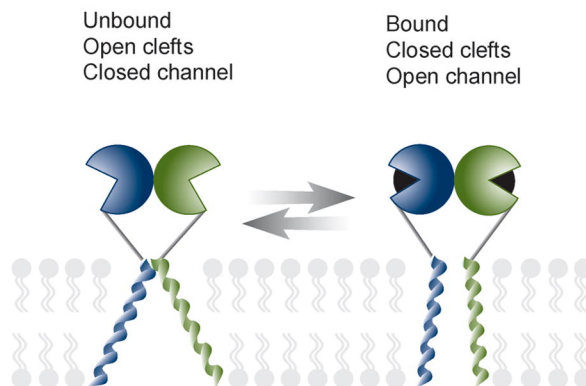


Figure 6



A

NR1-NR2



B

NR1-NR3

Unbound
Open clefts
Permissive NR1
Closed channel

Only NR3 bound
Open and closed clefts
Open channel

Bound
Closed clefts
Open channel

Desensitized
Closed clefts
Closed channel

